Knowledge-Based Systems 000 (2015) 1–14

Contents lists available at ScienceDirect

Knowledge-Based Systems

journal homepage: www.elsevier.com/locate/knosys

A keypoints-based feature extraction method for iris recognition under variable image quality conditions

Yuniol Alvarez-Betancourt, Miguel Garcia-Silvente*

CITIC-UGR. Department of Computer Science and Artificial Intelligence, University of Granada, Granada, Spain

ARTICLE INFO

Article history:
Received 6 May 2015
Revised 21 October 2015
Accepted 23 October 2015
Available online xxx

Keywords:
Biometrics
Iris recognition
Feature extraction
Local feature extraction
Information fusion
Keypoints

ABSTRACT

Iris recognition is a very reliable biometric modality for human identification. The immutable and unique characteristics of the iris are the foundations for that claim. Currently, research interest in this field points to challenges regarding less-constrained iris recognition systems. In response, we propose a robust keypoints-based feature extraction method for iris recognition under variable image quality conditions. To this end, three detectors have been used to identify distinctive keypoints: Harris-Laplace, Hessian-Laplace, and Fast-Hessian. Once the three sources of keypoints are obtained, they are described in terms of SIFT features. The proposed method combines the three information sources of SIFT features at matching score level. The combination of these sources reinforces the discriminative power of the proposal for recognition on highly or less textured iris images. The fusion is carried out using a proposed weighted sum rule relies on the ranking of three performance measures. The proposed fusion rule computes weights, which represent the reliability degree to which each individual source must contribute in order to determine the more discriminative matching scores. Our experiments rely on iris standard databases which as a whole constitute a challenging and perfect example of variable image quality conditions. According to the results, our proposal is very competitive and outperforms the state-of-the-art algorithms on the topic. In addition, it is demonstrated that the proposed keypoints-based feature extraction method is feasible and that it could be used even in real-time applications if the database is previously processed.

1. Introduction

In the last years, biometric technologies have arisen as the most reliable access control systems (e.g. fingerprints, hand geometry, face, ears, retina, and the iris) [28]. Among these biometric technologies, iris recognition has gained more popularity due to its characteristics: its rich texture is endowed with many degrees of freedom; it remains unchanged despite the aging process; it is protected by a structure which, if modified, may compromise the health of the individual, and it may be easily accessed with a non-invasive device [4]. Therefore, many leading companies in the field of security are betting on the future of this technology because of the diversification of its applications.

Currently, researchers in the field are faced with the challenge of non-ideal iris recognition [27,43,49]. Non-ideal iris recognition takes place in less constrained environments, which imply the relaxation of some factors such as: distance, person movements, lighting conditions [4]. In the literature we can find various surveys [4,9] which summarize novel approaches and trends in this field of research. A conventional iris recognition system consists of the 4 following stages: (1) image acquisition [28,33]; (2) preprocessing (spoofing detection [10]; image quality assessment [24]; iris segmentation [14,18,50]; and normalization [14]); (3) feature extraction [14,30,39,40,44,57]; and (4) pattern matching [14,39]. Roughly speaking, the process starts with the acquisition of the iris image and concludes with the decision to accept or reject the claimed identity.

The feature extraction stage has been studied in depth but it requires additional research in order to gain in robustness and accuracy. To a certain extent, this is due to the fact that recognition in less-constrained environments involves challenges concerning the quality of iris images such as: illumination, occlusion, blur, scale, rotation, point of view, etc., because they may produce severe texture deformations. The iris texture is characterized by the random distribution of local features such as: furrows, crypts, freckles, pigment spots and pigment frill. The success of both the iris segmentation and the feature extraction stages is closely related to the quality factors of iris images. The systems which are very dependent on texture details are the most prone to failure in the execution of these stages. Therefore, the global performance of the biometric system could be

* Corresponding author. Tel.: +34 958240807; fax: +34 958243317.
E-mail addresses: yuniol@decsai.ugr.es (Y. Alvarez-Betancourt), m.garcia-silvente@decsai.ugr.es (M. Garcia-Silvente).

http://dx.doi.org/10.1016/j.knosys.2015.10.024
0950-7051/

compromised. Consequently, iris feature extraction under variable image quality conditions remains a challenge worthy of investigation.

Until now, contributions to the topic of iris feature extraction have been based on two main approaches according to the type of representation of iris texture: binary iris code or real-valued feature vectors [9]. This is the most used classification of feature extraction methods in iris research. The work by Daugman [12] underlies the approach of the binary iris code. In that work, the binary iris code is obtained by means of an encoding process on phase information from a transformation of 2-D Gabor wavelets. Other studies obtain the binary representation using several transformations such as: a Hilbert transform [58], a dyadic wavelet transform [31], a 2D Log-Gabor filters [61], a discrete cosine transform [40], a 2D Fourier phase code transformation [39], and a multilobe differential filters [57]. As to the methods based on real-valued feature vectors, they use transformations similar to the ones mentioned previously, that is keeping the transformation output with the original real-valued feature vector. However, they do not go through a binary coding process. As examples of real-valued feature representations obtained with some transformations, let us mention: a 1D wavelet transform [8], a 1D dyadic wavelet transform [52], an independent component analysis [20], a symmetric Gabor filters [30], a principal component analysis [11], a Daubechies-4 wavelet packet decomposition [16], and a 2D weighted principal component analysis [63].

Another element to bear in mind is the way in which the feature extraction method is accomplished. This could be summarized under three main categories of iris feature extraction: (1) whole iris region based, (2) regions of interest based, (3) points of interest based. The first one corresponds to the traditional iris recognition systems where global and local features are extracted from the whole iris region [14,31,39,40]. The second one includes the methods which extract local features from regions of interest with the aim to overcome the shortcomings arising mainly from eyelashes and eyelids occlusions. As an example of these systems based on regions of interest, let us mention: the upper portion of a normalized iris image (corresponding to regions closer to the pupil) [30], the annular region before the normalization process [51], the sub-regions without occlusions in the normalized image [38], the six independent biometric signatures from different iris regions [43], the annular collarette area [48]. The third category deals with approaches based on points of interest, also named keypoints-based methods. The methods included in this category extract real-valued feature vectors which describe the appearance around each keypoint. To this end, the features extracted have to be invariant as to scale, rotation, illumination, noise, and viewpoint. The keypoints-based methods are very useful in object recognition applications on images disrupted by occlusion, clutter, or noise [59]. Several keypoints-based methods for iris recognition have been presented in past publications [2,6,15,34,35,47,54,56]. These methods perform well enough in the case of noised images but they still need improvement in terms of accuracy even in studies considered as being state-of-the-art.

That is why, convinced of the intrinsic advantages of the existing keypoints-based methods, we propose a new improved version based on the fusion of keypoints-based information sources. More specifically, our aim is to develop a keypoints-based feature extraction method which, thanks to its flexibility and characteristics, would allow more accuracy in the case of iris recognition under variable image quality conditions. Our proposal does not require conditions such as: accurate iris location, normalization of annular iris region (allowing removal of the aliasing problem [42]), and occlusion detection. We theorize that the strengths of keypoints-based feature extraction methods [59] can be very useful in the case of inaccurate segmentations as result of iris recognition on less-constrained environments. The proposal has the advantage of fusing information from different sources. The unimodal biometric applications are often affected by several practical problems like noisy sensor data, non-universality and/or lack of distinctiveness of the biometric trait, unacceptable error rates, and spoof attacks [21]. Hence the fusion of multiple sources or modalities is an efficient way to overcome them. The proposal combines the three keypoint sources at matching score level with a proposed weighted sum rule based on the ranking of three performance measures. Thereby, exhaustive experiments are developed in the verification and identification modes from which the respective performance measures and curves are obtained. The experiments rely on CASIA-IrisV4-Interval, MMU 2, and UBIRIS 1 databases which contain iris images with a great variability of image quality conditions. The results point to the innovative nature of our methodology.

The remainder of this paper is structured as follows: Section 2 explains how the iris is segmented for the subsequent extraction of the features. Section 3 provides the details of the proposed iris feature extraction method. The description of the experiments and the discussion of the results are presented in Section 4. Finally, in Section 5, we present the conclusions of our work.

2. Iris segmentation

The iris is an internal organ of the eye located behind the cornea and the aqueous humor. It consists of a weave of connective tissues, fibers, rings and colors which constitute a distinctive and unique mark of people. By observing the iris from the center of the circle which models the inner boundary up to its outer boundary, two delimiting borders can be identified (see Fig. 1(a)). The first one, pupil–iris border, is defined by the shift of the intensity lower values (pupil region) of the image to middle intensities which characterize the iris region. The second border, iris–sclera, is characterized by the shift of middle values of intensity to the highest values (sclera region) of the image. Also, its geometric shape (circular or elliptical depending on the point of view) constitutes another feature of great importance for automatic detection [4]. Taking as a base the previous assumptions, we segment the iris the way we did in our previous work [3], that is in two main stages. The first one obtain an initial approximation of the center $P(X_0, Y_0)$ of the iris region. This time, we propose a more accurate method to approximate the iris center. In the second stage, we try to find the circular boundaries from the obtained initial approximation of the iris center, which best represent the inner and outer boundaries of the iris. Overall, the quality of the segmentation stage is reliable on the success of the initial approximation of the iris center.

2.1. Initial approximation of the iris center

The approximation of the iris center starts from the assumption that it is very close to the center of the processed images. The assumption is supported by the fact that the majority of iris capture-devices extract a square region of each eye which are very close to the image center. The iris image databases used in our work are examples of that. The proposed method sets out to look for the biggest dark object in the image which stands for the pupil. Basically, we start an iterative procedure of profile operations from the image center $P(X_I, Y_I)$ (see Fig. 1(a)). The profile operations are executed for each point in the horizontal (denoted as H_P) and vertical (denoted as V_P) directions. The region within which are processed candidate points of the iris center corresponds to the square region delimited by the size $2mX2m$ with center in $P(X_I, Y_I)$ (see the dashed square region in Fig. 1(a)). It is worth noting that in a profile operation, pixel-values are obtained along straight line segments (in our case, lines are in the horizontal and vertical directions). Thereby, the iris center is represented by the point $P(X_0, Y_0)$ in which H_P and V_P have the same number of consecutive pixels lower than a threshold h. The white axes in Fig. 1(a) denote profiles which correspond to the iris center. Besides, Fig. 1(b)

Please cite this article as: Y. Alvarez-Betancourt, M. Garcia-Silvente, A keypoints-based feature extraction method for iris recognition under variable image quality conditions, Knowledge-Based Systems (2015), http://dx.doi.org/10.1016/j.knosys.2015.10.024

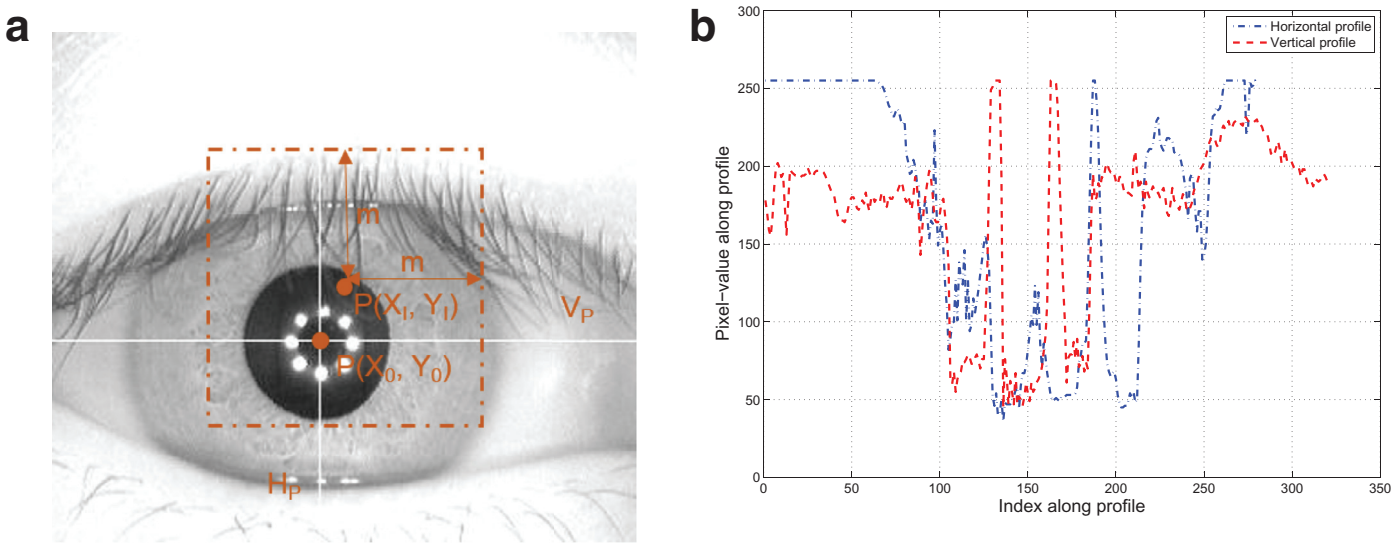

Fig. 1. (a) Graphical representation. (b) Chart with horizontal and vertical profiles corresponding to the iris center.

plots the index versus pixel-values along the profiles H_P and V_P corresponding to the iris center. We have determined experimentally that the best suited parameter values on the used iris image databases are $m = 70$ and $h = 50$.

2.2. Segmentation of inner and outer iris boundaries

In order to segment the inner and outer iris boundaries, two searches of circular boundaries are carried out. To find each one of the circular boundaries, we formulate a search problem as determining the radius $r_s^* \in R$, $R = \{r_{\min}, r_{\min}+1, \ldots, r_{\max}-1, r_{\max}\}$ of the circle with center $P(X_0, Y_0)$ such as:

$$r_s^* = \arg\max_{r \in R} D_s(r) \tag{1}$$

$$D_s(r) = \underset{(x_i,y_i)\in C_s(r,X_0,Y_0)}{F_{QMA}} \left(\frac{\partial f(x_i,y_i)}{\partial s} \right) = \underset{(x_i,y_i)\in C_s(r,X_0,Y_0)}{F_{QMA}} \left(f(x_i+\Delta_{sx_i}, y_i+\Delta_{sy_i}) - f(x_i,y_i) \right), \tag{2}$$

where F_{QMA} stands for the quantified majority operator QMA-OWA [3] and $f(x_i, y_i)$ is the intensity of a pixel of image F in coordinates (x_i, y_i). Also, $C_s(r, X_0, Y_0)$ is the set of m points of interest belonging to the semi circumference in the sense $s \in S$, $S = \{left, right, top, bottom\}$ such as:

$$C_{left}(r, X_0, Y_0) = \{(X_0 - r, Y_0)\} \cup$$

$$\{(x_i, y_i)/y_i = y_{i-1} \pm i; x_i = X_0 - \sqrt{r^2 - (y_i - Y_0)^2}\} \tag{3}$$

$$C_{right}(r, X_0, Y_0) = \{(X_0 + r, Y_0)\} \cup$$

$$\{(x_i, y_i)/y_i = y_{i-1} \pm i; x_i = X_0 + \sqrt{r^2 - (y_i - Y_0)^2}\} \tag{4}$$

$$C_{top}(r, X_0, Y_0) = \{(X_0, Y_0 - r)\} \cup$$

$$\{(x_i, y_i)/x_i = x_{i-1} \pm i; y_i = Y_0 - \sqrt{r^2 - (x_i - X_0)^2}\} \tag{5}$$

$$C_{bottom}(r, X_0, Y_0) = \{(X_0, Y_0 + r)\} \cup$$

$$\{(x_i, y_i)/x_i = x_{i-1} \pm i; y_i = Y_0 + \sqrt{r^2 - (x_i - X_0)^2}\}, \tag{6}$$

with $i = 1, \ldots, \frac{m}{2}$ where $m = 10$ and $m = 20$ for the detection of the inner and outer boundaries respectively. Besides, we set experimentally $r_{\min} = 20$, $r_{\max} = 70$ for inner boundary and $r_{\min} = 80$, $r_{\max} = 130$ for outer boundary on CASIA-IrisV4-Interval database. Also, we set $r_{\min} = 5$, $r_{\max} = 30$ for inner boundary and $r_{\min} = 40$, $r_{\max} = 70$ for outer boundary on MMU 2 and UBIRIS 1 databases. Fig. 2 shows some examples of successful iris segmentation on the three iris image databases used in our work.

3. Proposed iris feature extraction method

The flow chart of our proposal is depicted in Fig. 3. Once the iris is segmented according to the approach explained in the previous section, we can proceed with the proposed keypoints-based feature extraction method. In the context of multi-biometrics, our method can be classified as a multi-algorithm method which combines information from multiple sources at matching score level. To this end, we extract the iris region with the aim of reducing the processing time as is shown in Fig. 4(a). This means that we analyze only salient keypoints in the whole region delimited by the inner and outer circular boundaries, no matter the existing occlusions by eyelashes and eyelids. The occlusions are not detected because the keypoints-based feature extraction approaches remain robust in cluttered images [59]. Also, these occlusions belong to the periocular region which represents an alternative when iris recognition fails [7]. Consequently, we apply an efficient digital image processing technique in order to enhance the texture details of the iris region. In this enhanced image, we execute three keypoints detectors and for each one, the SIFT descriptor is used to obtain distinctive features from different information sources. Although using SIFT features for iris recognition is not novel, to our best knowledge, this is the first time that the potentialities of SIFT features are used to describes other sources of keypoints and fuse them to achieve a robust iris recognition under variable image quality conditions. Besides, a restrictive variant of the nearest neighbor distance ratio is proposed to compute the matching score between the target iris image and the enrolled iris image which are represented in terms of SIFT features. Moreover, a weighted sum rule for fusion at matching score level is proposed in order to increase the discriminative power of the individual sources. The weights for the proposed fusion scheme are determined using an approach based on the ranking of performance measures. In the following sections, we explain in more detail each of the steps mentioned for the proposed keypoints-based feature extraction method.

Please cite this article as: Y. Alvarez-Betancourt, M. Garcia-Silvente, A keypoints-based feature extraction method for iris recognition under variable image quality conditions, Knowledge-Based Systems (2015), http://dx.doi.org/10.1016/j.knosys.2015.10.024

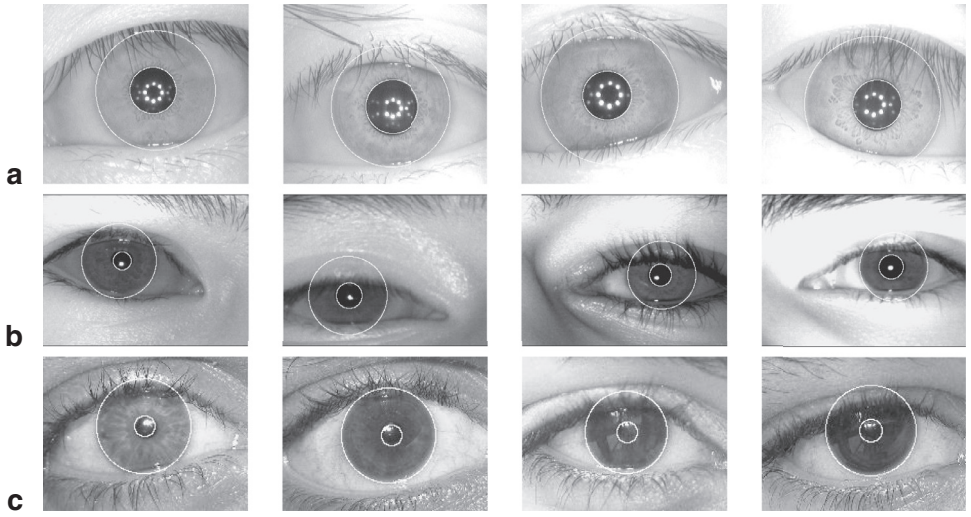

Fig. 2. Example of successful iris segmentation using the proposed method. (a) CASIA-IrisV4-Interval database. (b) MMU 2 database. (c) UBIRIS 1 database.

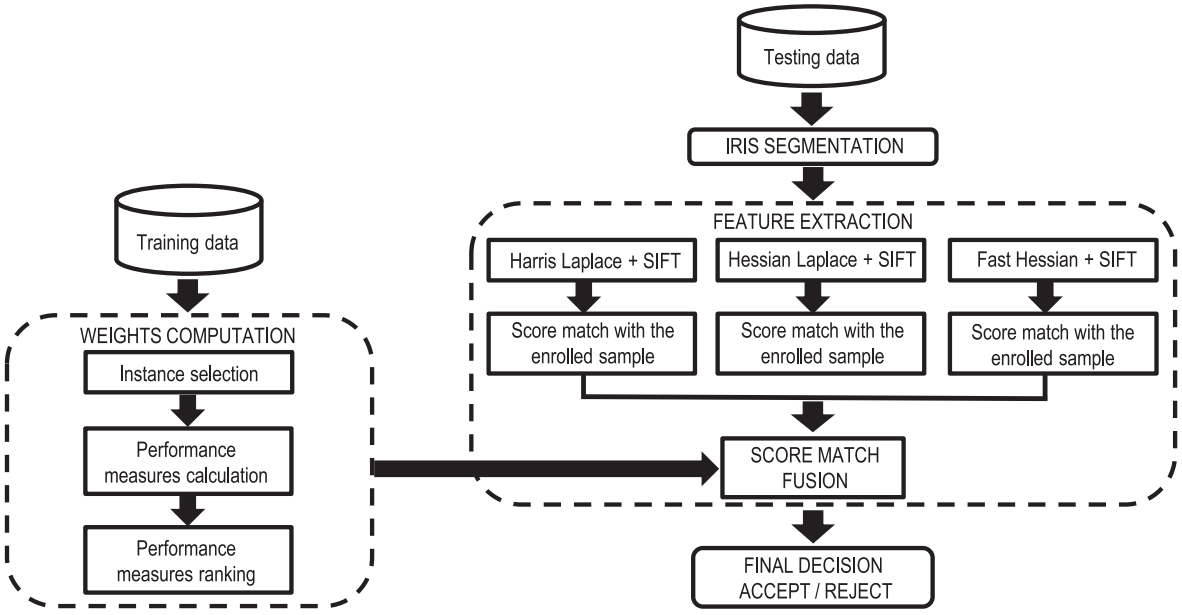

Fig. 3. Flow chart of the proposed keypoints based feature extraction method.

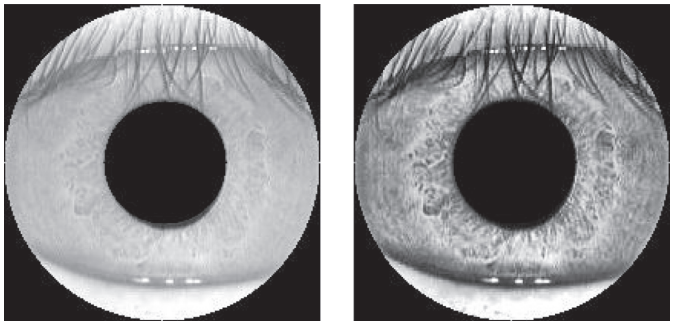

Fig. 4. (a) Raw image. (b) Results of adaptive histogram equalization.

3.1. Enhancing the iris texture

Iris texture is enhanced thanks to a popular method of contrast enhancement. The contrast-limited adaptive histogram equalization (CLAHE) method [64] enhances the contrast of grayscale images. The CLAHE method works on small neighborhood of 8×8 which are named tiles. This method enhances the contrast on tiles, so that the histogram of the transformed images approximately matches a Flat histogram. The neighboring tiles are then combined using bilinear interpolation to eliminate artificially induced boundaries. The contrast, especially in homogeneous areas, can be limited to avoid amplifying any noise that might be present in the image. Fig. 4(b) shows the result of applying this transformation to the raw image.

3.2. Feature extraction based on keypoints

The classical keypoints-based feature extraction methods are formed by the keypoints detector and the descriptor of the region around each detected keypoint. The keypoints detectors aim to detect mainly keypoints invariant to scale, point of view, and/or affine transformations [36]. They are based on the search for characteristics such as corners (Harris, Harris-Affine, Harris-Laplace, SUSAN), blobs (Hessian, Hessian-Affine, Fast-Hessian, Hessian-Laplace, Difference of Gaussian, Laplacian of Gaussian), and regions (MSER, IBR) [59]. The

Please cite this article as: Y. Alvarez-Betancourt, M. Garcia-Silvente, A keypoints-based feature extraction method for iris recognition under variable image quality conditions, Knowledge-Based Systems (2015), http://dx.doi.org/10.1016/j.knosys.2015.10.024

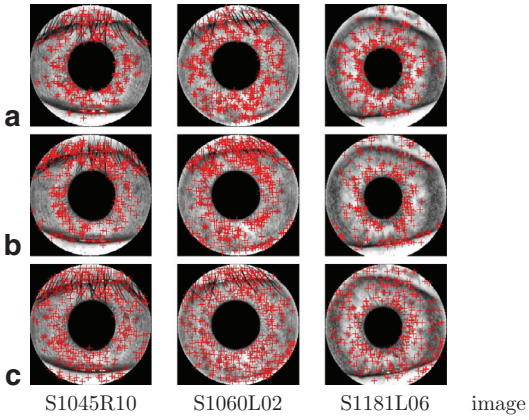

Fig. 5. Example of keypoints detection using different detectors on three images of the CASIA-IrisV4-Interval database. (a) Results for the Harris-Laplace detector. (b) Results for the Hessian-Laplace detector. (c) Results for the Fast-Hessian detector.

Table 1
Example, for three images, of the percentage of keypoints with enough quality with each detector.

	S1045R10	S1060L02	S1181L06
Harris-Laplace	82.25%	91.61%	96.34%
Hessian-Laplace	75.79%	78.85%	92.73%
Fast-Hessian	71.04%	83.43%	86.81%

purpose of the descriptors is to extract some distinctive information around each keypoint for matching and recognition. They are classified as follows: distribution-based descriptors (SIFT, PCA-SIFT, GLOH, SURF), spatial-frequency techniques (Fourier transform, Gabor transform, Wavelet transform), and differential descriptors (Steerable filters, Differential invariants) [37].

Based on the documentation related to these detectors and descriptors as well as the results of previous research [36,37,59], we have carried out several experimental tests with the purpose of selecting a well-suited combination of a few detectors and a descriptor for iris recognition. The experimental tests were developed on the three iris image databases used in our work and rely on several available source codes[1,2] and other self-developed source codes with parameter values recommended by different authors. After having tried several combinations of keypoint detectors and descriptors, we have decided that it might be wise to investigate the combined use of a corner-based detector Harris-Laplace and the two blob-based detectors Hessian-Laplace and Fast-Hessian. The success of the corner-based detector depends mainly on highly textured images while the blob-based detectors require less textured images to extract distinctive keypoints. This combination of information sources is adequate to complement the discriminatory power of the individual sources.

Fig. 5 shows the result of keypoints detection on three iris images of CASIA-IrisV4-Interval database using the three keypoints detectors selected in our study.

Table 1 shows the percentage of detected keypoints with enough quality in respect to the total number of detected points. The quality term means that keypoints detected in the eyelid regions are less useful than the keypoints detected in iris regions. The results indicate that even in the most occluded iris images the 3 used keypoints detectors are not biased by artifacts in eyelid regions such as reflections.

Besides, we have selected the SIFT method as feature descriptor because according to our previous experience, of all the experimented feature descriptors, it is the most adequate to support the selected key points detectors. This descriptor underlies several variants of descriptors and has proven to be very robust compared to other descriptors in other recognition applications [37]. We have to admit that the SIFT descriptor has been criticized for being a time-consuming technique. However, no other descriptor significantly surpasses it in terms of robustness and efficiency. In our work, we propose a new design to make it more suited for recognition on large databases.

3.2.1. Operators

The Harris-Laplace operator is a corner-based keypoints detector which is invariant to rotation and scale changes [36]. Several studies have shown that Harris-Laplace can reach high repeatability and localization accuracy in comparison with other invariant-scale detectors. However, its scale estimation is less accurate due to the multi-scale nature of the Harris corners detector [59]. The Harris-Laplace operator combines the Harris detector and the scale selection approach based on the Laplacian function [59].

The Hessian-Laplace detector is a blob-based operator used to detect keypoints in an image which is invariant to rotation and scale changes [59]. This detector was conceived with the same general idea as the Harris-Laplace detector. This means that Hessian-Laplace exploits the potentialities of the combination of the Hessian detector and the scale selection approach based on the Laplacian function. Hessian-Laplace is more robust than the Hessian detector because blob-like structures are better localized in scale than in corners and the detector benefits from multiscale analysis although it is less accurately localized in the image plane [59]. The Hessian-Laplace detector determines the location of the keypoints by the detection of the local maxima in the 8-neighborhood of a point x at each level of representation.

The Fast-Hessian detector is a blob-based operator designed to detect keypoints in an image. This operator is a scale-invariant feature detector based on the approximation of the Hessian matrix. Also, it uses the concept of integral images to efficiently compute a rough approximation of the Hessian matrix. The Fast-Hessian detector was first introduced by Bay et al. as a fundamental part of the SURF method (Speeded Up Robust Features) [5].

The approximated determinant of the Hessian represents the blob response in the image at location x. These responses are stored in a blob response map over different scales, and the local maxima is detected as a result of an interpolation operation.

3.2.2. SIFT keypoints descriptor

The Scale invariant feature transform method (SIFT) provides a robust keypoint descriptor and was proposed by Lowe [29] for image point matching. The features extracted by SIFT are invariant to image scale and rotation, and are shown to provide robust matching across a substantial range of affine distortion, change in 3D viewpoint, addition of noise, and change in illumination [29]. This descriptor builds a vector containing the values of all orientation histogram entries in the region around each keypoint. These orientation histogram entries are determined from the gradient magnitude and orientation around each keypoint. Besides, the gradient magnitude and orientation are weighted by a Gaussian window as can be seen on the left side of Fig. 6. Although the right side of Fig. 6 shows a 2×2 array of histograms computed from a 8×8 set of samples, the best results are obtained with a 4×4 array of histograms with 8 orientation bins in each [29]. As a result, the descriptor is formed by a real-valued vector of dimension $4\times4\times8 = 128$.

Finally, the real-value vector which characterizes the descriptor is modified in order to reduce the effects of affine illumination changes. First, the real-value vector is normalized to unit length and later it is thresholded to values larger than 0.2. Also, the vector is renormalized to unit length. This means that matching the magnitudes for large

[1] LIP-VIREO toolbox (http://www.cs.cityu.edu.hk/~wzhao2/lip-vireo.htm).
[2] VLFeat toolbox (http://www.vlfeat.org).

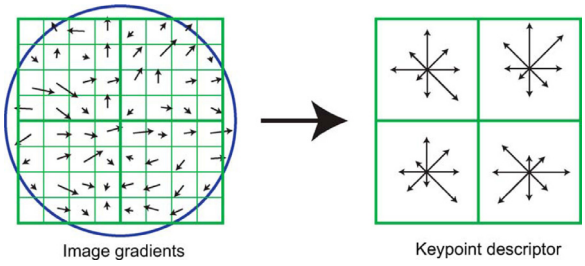

Fig. 6. Graphical representation of the SIFT descriptor computation. This picture was taken from [29].

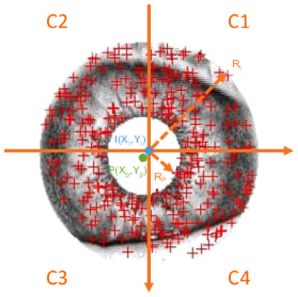

Fig. 7. Graphical representation of the division of iris region in 4 quadrants.

gradients is no longer important, and that more emphasis is placed on the distribution of orientations.

3.2.3. Matching

A target iris image will be classified as an instance of the class X, if its largest number of matches corresponds to any enrolled iris image of the X class. The nearest neighbor distance ratio was used to compute the number of matches between two images which are represented in terms of SIFT features [29]. In addition, we have introduced a location constraint to prevent false matches and to reduce the computational time required to match SIFT based features from the three used information sources. To this end, we have divided the iris region into 4 quadrants to execute comparisons only among keypoint descriptors of the same quadrant (see Fig. 7). This kind of restriction is based on the premise that similar keypoint descriptors of two images are situated in the same quadrant in spite of the resolution and rotation variations of the images. It is important to stress that the proposed location constraint works well on the matching of real iris images affected by image rotation. In real applications, iris images are captured on people which are walking erect and thus the image rotation is not significant. In the following, we will present the definition of each quadrant in more detail:

$$C1 : [X_P + 1, X_I + R_I][Y_I - R_I, Y_P]$$
$$C2 : [X_I - R_I, X_P][Y_I - R_I, Y_P]$$
$$C3 : [X_I - R_I, X_P][Y_P + 1, Y_I + R_I]$$
$$C4 : [X_P + 1, X_I + R_I][Y_P + 1, Y_I + R_I]$$

This distance is very useful in the case of matching two iris images that have occlusions. This statement is based on the fact that by matching two images using the nearest neighbor distance ratio we will only find matches in the iris regions. For example, all iris images from the same individual have in common the texture of iris region which is delimited by several kinds of eyelids occlusions. As a general rule, the iris images captured from the same individual in different sessions, do not have very similar eyelid regions. Hence, the final quantity of similitude between two images always refer to the textural content on the iris region and it includes in a few rare cases some similitude on eyelid regions. Besides, we have identified the possible cases where matches can be found:

- comparing a clear iris image with an occluded iris image from the same individual (the matches are found only on both iris regions).
- comparing two iris images with a different degree of occlusion from the same individual (the matches are found only on both iris regions).
- comparing two iris images with a similar degree of occlusion from the same individual (the matches are found on both iris regions and on similar occluded regions).

3.3. Information fusion from multiple sources

Information fusion deals with the aggregation of evidence provided by multiple sources of information (sensors, algorithms and so on) with the aim to make a decision [46]. In biometrics, the fusion of information from multiple biometric modalities is catalogued as multi-biometrics. This discipline constitutes a very efficient approach when unimodal biometric applications are affected by practical problems such as noisy sensor data, non-universality and/or lack of distinctiveness of the biometric trait, unacceptable error rates, and spoof attacks [21]. Several applications have included information fusion from different sources or algorithms in order to increase its global performance in an effective way. As examples, we can mention: multi-modal biometric systems [21], image annotation [62], hierarchical cluster ensemble selection [1], classifier ensemble framework [41], and pedestrian detection [17].

The multi-biometric systems can be classified into one of six categories based on the nature of the sources [46]. These categories are: (1) multi-sensor (e.g. 2D and 3D face sensors); (2) multi-algorithm (e.g., binary iris code based and real-valued feature vectors based iris matchers); (3) multi-instance (e.g. left and right irises); (4) multi-sample (e.g. capturing several instances of the iris in different sessions); (5) multi-modal (e.g. iris and fingerprint); and (6) hybrid (e.g combinations of any of the previous approaches). Besides, several levels of fusion are defined according to the information available in a certain module of a multi-biometric system. These levels of fusion are grouped in two broad categories: pre-classification or fusion before matching (sensor level, feature level), and post-classification or fusion after matching (matching score level, rank level, or decision level) [53].

The fusion at the matching score level is one of the most used approaches because it is natural, simple and fast. The score combination is a more natural process, and it is well suited to implement real time applications. Given that the matching score outputs by the various modalities are heterogeneous in some cases, score normalization is needed to transform these matching scores into a common domain, prior to combining them [21]. Besides, a great variety of fusion methods has been proposed. They are classified in two categories: supervised and unsupervised methods. The supervised methods are more complex because they require prior knowledge (training data). Also, these methods require that a multi-categorical problem be transformed into a two-category problem (genuine and impostor classes) when a challenge imbalance class problem arises. The imbalance class problem is characterized as having many more instances of certain classes than others. This problem is usually discussed as two-category problems where one class is represented by a large set of samples while the other one is represented by only a few. In the context of biometrics, the distribution of samples per subject in the majority of image databases is low and the number of subjects is high. We deal with a two-category imbalance class problem when in almost all cases the genuine class represents 1% and the impostor class represents 99% of all samples. Therefore, a classifier will find it more difficult to predict classes with few samples and consequently the test samples of this class will more often be misclassified than the test samples of the prevalent class. An alternative method to remedy this problem is presented in [21]. In that study, the used data are represented by 1000 genuine score vectors and 49,000

Please cite this article as: Y. Alvarez-Betancourt, M. Garcia-Silvente, A keypoints-based feature extraction method for iris recognition under variable image quality conditions, Knowledge-Based Systems (2015), http://dx.doi.org/10.1016/j.knosys.2015.10.024

impostor score vectors. In order to train the classifier to perform his task, an under-sample model of instance selection is used, based on the random selection of 6 genuine and 6 impostor score vectors for each user. The most frequently used techniques in the supervised methods are support vector machines, decision trees, linear discriminant analysis, and classifier ensembles [21]. The unsupervised methods are less complex and very efficient. Some of them (e.g. Product rule, Sum rule, Min rule, Max rule, Median rule, and Majority voting) have been extensively experimented within the common theoretical framework for classifier combination presented by Kittler et al. [25]. In that work, the superiority of the Sum rule was proven. Subsequently, it was shown that the Sum rule was overcome by the weighted sum rule of scores [21]. This rule uses user-specific weights from the different modalities which involve a more complex learning process. All these elements have motivated the proposed fusion scheme which is more efficient and easy to use. It is worth noting that in our work, the used information sources are homogeneous, and consequently matching score normalization [21] is not required. In the next section we will provide a more detailed explanation of the proposed fusion scheme.

3.3.1. Proposed fusion scheme

Our proposed fusion scheme is based on the weighted sum rule of matching scores from different sources. We consider it an effective and reliable approach to compute the weights of each source which make up the final matching score of each test sample. This approach arises from the assumption that the more reliable information source is the one which best satisfies all the established objectives in a specific context. It is also assumed that the source which best satisfies an objective receives the highest value of the ranking (corresponding to the number of sources n). On the other hand, the source which least satisfies an objective receives the lowest value of the ranking (corresponding to the first position 1). This approach which consists in the ranking of objective satisfaction for each source is denoted as reverse rank position. Generally speaking, we consider that the value v_{ij} obtained when the j-th measure is applied to the i-th source, with $1 \le i \le n$ and $1 \le j \le m$. σ_i is a permutation such as: $v_{i\sigma_i(j)} < v_{i\sigma_i(j+1)}$ for all $1 \le j < m$. So, we define the reverse rank position such that $p_{ij} = (n+1) - \sigma_i(j)$ and is based on the position indicated by σ_i in the order of objective satisfaction denoted by the measure j. Accordingly, an accumulated rank (γ_i) of the i-th source is defined as the sum of its corresponding values of p_{ij} in the ranking of satisfaction for each formulated objective. Finally, the weight corresponding to a source is the proportion of its accumulated rank with respect to the total accumulated rank of the n sources. It is worth noting that the weights are conceived in the range [0, 1] and their sum is equal to 1. These two properties raise the confidence level in the computed weights of relevance for each source. A formal definition of our proposed fusion scheme is provided in the following aggregation function.

Definition. The aggregation function of dimension n is a mapping $F : \mathbb{R}^n \to \mathbb{R}$ that has an associated vector of weights $W = (w_1, \ldots, w_n)$ such that, $w_i \in [0, 1]$, $1 \le i \le n$, and $\sum_{i=1}^{n} w_i = 1$, and they are defined as follows:

$$w_i = \frac{\gamma_i}{\gamma_T}, \tag{7}$$

with

$$\gamma_i = \sum_{j=1}^{m} p_{ij}, \tag{8}$$

and

$$\gamma_T = \sum_{i=1}^{n}\sum_{j=1}^{m} p_{ij} = \sum_{i=1}^{n} \gamma_i, \tag{9}$$

Table 2
Weights computed for a case of fusion of 4 information sources with respect to 3 objectives.

	Objective 1	Objective 2	Objective 3	γ_i	w_i
Source 1	7 (3)	2 (3)	5 (2)	8	0.27
Source 2	4 (1)	5 (2)	9 (4)	7	0.23
Source 3	10 (4)	8 (1)	2 (1)	6	0.20
Source 4	6 (2)	1 (4)	7 (3)	9	0.30
γ_T				30	–

where $p_{ij} = (n+1) - \sigma_i(j)$ is the i-th reverse rank position of source i with respect to the j-th objective.

Finally, the aggregation function will be:

$$F(x_1, x_2, \ldots, x_n) = \sum_{i=1}^{n} w_i S_i, \tag{10}$$

where S_i is the matching score corresponding to the i-th information source.

Table 2 shows the computed weights for a general problem of information fusion of 4 information sources which must satisfy 3 objectives. In this case, each information source is represented by a vector of four values in the range [0, 10]. Each value of the i-th vector represents each objective. As to the objectives, Objective 1 and Objective 3 stand for objectives to be maximized and Objective 2 must be minimized. In brackets, we show the reverse rank position p_{ij} for which each information source satisfies each objective. Thereby, the weights are presented clearly.

Here, we propose the use of performance measures of each individual information source as objectives to be satisfied. The performance measures could be determined in two modes: verification and identification. The verification mode is conceived for positive recognition, when the goal is to prevent different people from using the same identity [22]. In that mode, the system performs a one-to-one matching to determine whether the claim is true or not. To this end, the claimed identity of a person X_l presented to the system as a template is matched with the claimed person template E_l. Thus if the degree of similarity $D(X_l, E_l)$ (e.g. compared with the nearest neighbor distance ratio like in this work) is higher than a threshold T_0, then the claim is accepted; otherwise, the claim is rejected (or vice versa if another measure of similarity is used). The commonly used performance measures are:

- false accept rate (*FAR*) stands for the percentage of verification transactions with wrongful claims of identity that are incorrectly confirmed,
- false reject rate (*FRR*) indicates the percentage of verification transactions with truthful claims of identity that are incorrectly denied, and
- genuine accept rate ($GAR = 100 - FRR$).

These measures can be plotted against all possible values of T_0, resulting in the so-called performance curves. The receiver operator characteristic (ROC) curve plots *FAR* against genuine accept rate *GAR*. The area under the ROC curve (AUC) is another useful performance measure which provides a good summary for comparing ROC curves [19]. Furthermore, the detection error trade-off (DET) curve, is the graph of *FAR* against *FRR*. Besides, the equal error rate (*EER*) is another useful measure which represents the value whenever *FAR* and *FRR* are equal.

The identification mode is envisaged for negative recognition applications which prevent an individual from using multiple identities [22]. In this mode, the system performs one-to-many matching between the claim of a person's identity X_l presented to the system and all the enrolled identity. This process allows to determine which

matching between an enrolled person template E_l and the input template reaches the minimal degree of dissimilarity $D(X_l, E_l)$ (e.g. compared with the nearest neighbor distance ratio). To this end, the preferred identity corresponds to the minimal $D(X_l, E_l)$ which must be higher than a predefined threshold T_0 (i.e. to face the fact that the input template corresponds to a non-enrolled person) as well. Furthermore, the metric correct recognition rate (*CRR*) at rank k is used to measure the performance in that mode (e.g the most used value for k is 1). The *CRR* at *Rank-k* represents the percentage of times the correct identities of the tested identities are among the top k ranked matches. As performance curve in this mode, the cumulative match characteristic (CMC) curve is used to depict the variations of the *CRR* at *Rank-k* measure. The CMC curve plots *Rank-k* against the *CRR* rate.

In our study, we have decided to maximize the AUC, to minimize the EER, and to maximize the CCR at Rank-one which are the performance measures most frequently used to assess the performance of a biometric system. Besides, these measures are the most appropriate to assess the discriminative power of each individual source. Once the performance measures have been individually determined on each source, they are used to compute the weights which will address the fusion of matching scores for each test sample (see the flowchart presented in Fig. 3). The performance measures are computed only on the training data for each individual information source. This means that weights are computed in each data partition on the training data and before test samples were evaluated. First, an instance selection process on the training data is executed with the aim to compute the weights on the more discriminative instances of each information source. This process discards less-relevant instances such as represent images with poor quality or for which the extracted features are not discriminant enough. The proposed instance selection method is a kind of noise filter procedure based on the k nearest neighbors approach [23]. This procedure entails removing from the training data the instances whose its $k-1$ nearest neighbors do not belong to its class. In this case, the k value is variable and it is determined by the number of instances in the class which belong each checked instance. The procedure is execute on each information source and if an instance does not fulfill the above-mentioned condition, then it is removed from each information source.

To this end, the performance measures for weight estimation are based on the recognition performance of the nearest neighbor classifier with the proposed restrictive nearest neighbor distance ratio. The recognition performance is assessed through the k-fold cross-validation procedure in order to examine the performance of the classification in an unbiased way. This is suitable because the number of samples by class in each iris image database is limited [49]. In the k-fold cross-validation procedure, the database is partitioned into k subsets (folds) of approximately equal size. Hence, $k-1$ folds are used for training and the excluded fold is used for testing. This process is repeated for $k=3$ times, leaving one different fold for testing each time. The 3-fold cross-validation procedure enables us to improve the reliability of the discriminative power provided by each individual source. Hence the performance measures obtained in each fold are averaged to get a single indicator in each data partition; then weights for each individual source are calculated. The computed weights represent the reliability degree to which each individual source must contribute in order to determine the more discriminative matching scores.

4. Experiments and results

In this section, we present a protocol of experiments intended to validate the proposed feature extraction method for iris recognition. The experiments were executed on Matlab R2012b using a Core 2 Duo laptop computer at 2.2 GHz with 4 GB of RAM memory on the databases CASIA-IrisV4-Interval, MMU 2, and UBIRIS 1. First, we decided to conduct a statistical analysis in order to assess the complementary and discriminatory power of each information source having as base some concepts proposed in [60]. This statistical analysis enables us to validate the suitability of the fusion of the used information sources. Besides, we compared the recognition performance obtained when using individual sources with the recognition performance when using several basic fusion rules as well as the proposed fusion scheme. In this way, we can check what is the most suitable form of fusion for the used information sources in relation to our proposed fusion scheme. The experiments were developed using both a verification and identification mode. In the end, our proposed feature extraction is compared with state-of-the-art methods. In order to ensure the validity of the comparison, we strictly followed the same experimental conditions as the ones used in our work (e.g, hardware, system, data, iris segmentation method, classification approach). In addition, we present some results of time-consuming tests with the aim to demonstrate the suitability of the proposed feature extraction method with respect to the state-of-the-art methods to implement real applications.

4.1. Databases

We used three well-known image databases acquired in different spectrums of light. Several image databases are available for research [9,28], but the three we selected are those most commonly used because of their variability in both image quality factors and ethnicity. These databases as a whole constitute a perfect example of variable image quality conditions and hence enable us to develop the required experimentations in order to achieve the main objective defined in our work.

Description of the three databases:

- The CASIA-IrisV4-Interval database[3] is provided by The Chinese Academy of Sciences – Institute of Automation (CASIA), China. The images were collected from Asian individuals and were captured in the near infra-red spectrum using a specialized digital optics developed by CASIA. The images have a resolution of 320x280 pixels. The image database is affected by eyelash occlusions, eyelid occlusions, specular reflections, and illumination changes. The images from each individual were taken from right and left eyes in two sessions with one month interval between sessions. The CASIA-IrisV4-Interval contains 2639 gray scale eye images from 249 individuals.
- The MMU 2 database[4] is provided by the Multimedia University, Malaysia. The iris images were collected from natives of Asia, the Middle East, Africa, and Europe. These images were captured in the near infra-red spectrum using a Panasonic BM-ET100US Authenticam camera. The resolution of the iris images is 320 × 238. This image database is disrupted by eyelash occlusions, eyelid occlusions, glass occlusions, and specular reflections. The MMU 2 consists of 995 iris images from 100 individuals. Each of them contributed 5 iris images for each eye. The supplier has eliminated 5 left eye iris images from the database due to cataract disease.
- The UBIRIS 1 database[5] is provided by the SOCIA Lab at the University of Beira Interior, Portugal. The images were collected from Europeans and were captured in the visible spectrum with a Camera Model Nikon E5700. The acquisition process was developed within two distinct sessions characterized by different types of noise, simulating images captured with none or minimal collaboration from the subjects. The database is composed of 1877 color images collected from the right eye of 241 people. Three versions of the database are available depending on the resolution: 800 × 600 – 24 bit color, 200 × 150 – 24 bit color and 200 × 150

[3] Publicly available at CASIA website (http://biometrics.idealtest.org).
[4] Publicly available at MMU website (http://pesona.mmu.edu.my/~ccteo).
[5] Publicly available at UBIRIS website (http://iris.di.ubi.pt/ubiris1.html).

Please cite this article as: Y. Alvarez-Betancourt, M. Garcia-Silvente, A keypoints-based feature extraction method for iris recognition under variable image quality conditions, Knowledge-Based Systems (2015), http://dx.doi.org/10.1016/j.knosys.2015.10.024

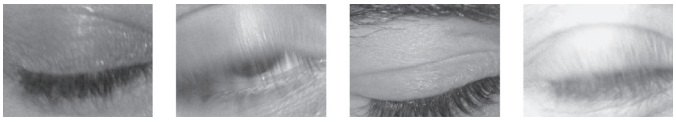

Fig. 8. Example of images from UBIRIS 1 database which are discarded in our experimentations.

Table 3
Spearman's correlation coefficients among the information sources.

	CASIA-IrisV4-Interval		
	Harris-Laplacian	Hessian-Laplacian	Fast-Hessian
Harris-Laplacian	1	0.1221	0.1619
Hessian-Laplacian	0.1221	1	0.2682
Fast-Hessian	0.1619	0.2682	1
	MMU 2		
Harris-Laplacian	1	0.0937	0.1161
Hessian-Laplacian	0.0937	1	0.2610
Fast-Hessian	0.1161	0.2610	1
	UBIRIS 1		
Harris-Laplacian	1	0.1082	0.1226
Hessian-Laplacian	0.1082	1	0.1583
Fast-Hessian	0.1226	0.1583	1

– Grayscale. Although the most frequently used version is 800 × 600 – 24 bit color, we have selected the version 200 × 150 – Grayscale because the recognition of very noised images is more challenging in images with low resolution. A set of 28 images had to be excluded manually from the experiments because they presented a complete or nearly complete occlusion of the iris (for an example of these images, see Fig. 8).

4.2. Statistical analysis of the information sources

A statistical analysis was conducted in order to demonstrate the strength of the selected information sources and of their combinations. This analysis had a double objective: assessing both the complementary and discriminatory power of the information sources. The complementary power was estimated by determining the statistical correlation among the information sources. This kind of analysis enables us to identify the degree of similarity among the information sources and therefore to pinpoint the sources which will provide the most relevant information. Analyzing the discriminatory power of each information source and their combination allows us to judge the degree of reliability of these sources for the recognition process. An ideal information source for iris recognition must be able to discriminate perfectly between his genuine and impostor score distributions. This would be the case of information sources with statistically significant differences between their respective genuine and impostor score distributions.

4.2.1. Complementary power

The complementary power was analyzed by means of Spearman's rho correlation coefficient [55]. Spearman's rho is one of the most widely used correlation coefficients to measure the degree of association between two or more variables. This claim is mainly supported by the fact that this correlation coefficient requires fewer computations and is appropriate for large data sets. Table 3 shows the correlation coefficients for the information sources used. The coefficients were calculated for pairs of matching score distributions of the information sources on each database. The coefficients are defined in the range [0, 1] such that a correlation value close to 0 means that the correlation is weak and a correlation value close to 1 means that it is strong.

Table 4
Kruskal–Wallis ANOVA statistics.

	CASIA-IrisV4-Interval			
	SS	MS	Chi-sq	PValue
Harris-Laplace	2.5957e+16	2.5957e+16	7.0537e+04	0.000
Hessian-Laplace	2.5120e+16	2.5120e+16	3.9697e+04	0.000
Fast-Hessian	2.5311e+16	2.5311e+16	2.5522e+04	0.000
	MMU 2			
Harris-Laplace	5.6709e+13	5.6709e+13	1.7519e+04	0.000
Hessian-Laplace	5.5507e+13	5.5507e+13	7.2556e+03	0.000
Fast-Hessian	5.9189e+13	5.9189e+13	4.7879e+03	0.000
	UBIRIS 1			
Harris-Laplace	2.8622e+14	2.8622e+14	3.1312e+04	0.000
Hessian-Laplace	3.0172e+14	3.0172e+14	2.3536e+04	0.000
Fast-Hessian	3.4248e+14	3.4248e+14	7.5724e+03	0.000

In Table 3 we can observe that the highest correlation value is 0.2682, which is less than the 1/3 of the range of Spearman's rho correlation coefficient. This enables us to conclude that all the information sources are practically uncorrelated; therefore they can contribute different and useful information to our proposed iris feature extraction method. In the three databases, the least correlated sources are Harris-Laplace and Fast-Hessian. On the other hand, the most correlated sources are Fast-Hessian and Hessian-Laplace.

4.2.2. Discriminatory power

The analysis of the discriminatory power of the information sources starts with a one-way analysis of variance (ANOVA). The analysis of variance consists of inferential statistical procedures intended to evaluate the difference between at least two means in a set of data for which two or more means can be computed [55]. The classical procedure of one-way ANOVA requires the assumption of normality in the genuine and impostor score distributions for each source. The Kolmogorov–Smirnov goodness-of-fit test commonly used to test the normality assumption is very reliable in the case of large samples. In our experiments, it turned out that neither the genuine nor the impostor score distributions for each source fulfills the normality assumption. In all cases, the null hypothesis H0 (the data come from a standard normal distribution) was strongly rejected with a $pvalue = 0$ at 5% significance level. This entails the use of the Kruskal–Wallis test which is a nonparametric version of the classical one- way ANOVA [55]. Table 4 presents some statistics from the Kruskal–Wallis test for ANOVA. For each source, on each database Table 4 presents the following statistics: sum of squares (SS), mean squares (MS), chi-square statistic (Chi-sq) and significance of the chi-square statistic (PValue).

As can be seen in Table 4, the PValues are inferior to 0.005 for each information source in all the databases. This means we can strongly reject the null hypothesis H0 (the medians of both populations are equal) at 5% significance level. These results lead us to confirm that the genuine and impostor score distributions for each information source used in our study have statistically significant differences.

In addition, a classifier based on Linear Discriminant Analysis (LDA) was used to recognize the iris patterns from different sources and the fusion of them. As was explained in the previous section, the LDA classifier represents a typical supervised method for information fusion and this time it was used for fusion of information sources in a raw way. The recognition process was developed on samples represented by vectors of matching score values for each information source. The performance of the classifier LDA was examined by means of the holdout cross-validation procedure. In that procedure, 60% of the data is used for training and the remaining 40% is used for testing. In order to obtain a single indicator for each fold, the performance measures obtained are averaged. Thereby, each table presented below includes performance measure values

Please cite this article as: Y. Alvarez-Betancourt, M. Garcia-Silvente, A keypoints-based feature extraction method for iris recognition under variable image quality conditions, Knowledge-Based Systems (2015), http://dx.doi.org/10.1016/j.knosys.2015.10.024

Table 5
Performance measures of recognition using individual and combined information sources.

	CASIA-IrisV4-Interval		MMU 2		UBIRIS 1	
	AUC	EER	AUC	EER	AUC	EER
Harris-Laplace	98.70 ± 0.104	3.40 ± 0.006	97.79 ± 0.065	5.99 ± 0.003	86.59 ± 0.011	20.69 ± 0.007
Hessian-Laplace	98.54 ± 0.208	4.68 ± 0.002	96.74 ± 0.089	7.82 ± 0.014	88.49 ± 0.020	17.76 ± 0.008
Fast-Hessian	98.30 ± 0.517	5.26 ± 0.047	98.52 ± 0.116	5.52 ± 0.037	90.62 ± 0.141	17.47 ± 0.053
Combined	99.27 ± 0.103	2.37 ± 0.024	99.31 ± 0.062	3.00 ± 0.004	93.22 ± 0.046	13.65 ± 0.013

in the format: mean value ± standard deviation. The four classification schemes have used the same data partitions for training and testing the classifier. Table 5 presents some performance measures related to the analysis of the discriminatory power. Although the scheme combination is roughly applied, we can observe that the combination of the information sources used in our work is appropriate. This suggests that the discriminatory power of the individual information sources could be significantly enhanced by fusing them.

4.3. Performance evaluation of the proposed method

The performance evaluation of the proposed method was assessed in both the verification and identification modes. In addition, we compare the recognition performance of our proposal with the recognition performance using the individual sources as well as the three most notable fusion rules (i.e. Min rule, Max rule, and Sum rule) on the individual sources. The performance in the verification mode is presented by means of ROC curves which explicitly show the AUC values of each curve corresponding to each method. We also illustrate the performance of our proposal in the identification mode through the use of CMC curves which specify the respective values of CRR at Rank-one for each curve corresponding to each method.

To this effect, we have used the nearest neighbor classifier with the proposed restrictive nearest neighbor distance ratio. This allows us to evaluate the recognition performance using training data, which improves the performance of the proposed method. The k-fold cross-validation procedure has been used in order to examine the performance of the classification in an unbiased way. This involves a number of comparisons (NC) for each fold in each database with n amount of images where $NC = \frac{2n}{3} * \frac{n}{3} = \frac{2n^2}{9}$. It is worth noting that this experimental design was also used to assess the recognition performance of the individual sources and the standard fusion rules.

The next experiment deals with the comparison of recognition performance with individual sources, combined sources with Min rule, combined sources with Max rule, combined sources with Sum rule, and combined sources with proposed weighted sum rule in the verification mode on the three iris image databases. Fig. 9 shows the comparison through the use of ROC curves.

Our proposed method improves the recognition performance with the individual sources and the other fusion rules on the three databases. The best performance obtained by our proposal in terms of AUC is 99.90% on the CASIA-IrisV4-Interval database, 99.89% on the MMU 2 database, and 99.05% on the UBIRIS 1 database. In all databases, the best performance results are closely followed by the recognition performance on the use of Min rule and Sum rule. The worst performance is characterized by values of AUC of 99.69% with the individual source Hessian-Laplacian on the CASIA-IrisV4- Interval database, 98.55% with the individual source Hessian-Laplacian on the MMU 2 database, and 97.39% with the fusion by Max rule on the UBIRIS 1 database.

As to comparisons in the identification mode, Fig. 10 presents CMC curves of recognition performance in identification mode on the three iris image databases. As in the previous experiment, we compare the recognition performance of individual sources, combined sources with Min rule, combined sources with Max rule, combined sources with Sum rule, and combined sources with the proposed weighted sum rule.

In the experiments on the three databases, our proposed method surpasses the recognition performance with the individual sources and the other fusion rules. This is characterized by values of CRR at Rank-one of 99.20% on the CASIA-IrisV4-Interval database, 98.08% on the MMU 2 database, and 89.41% on the UBIRIS 1 database. The Sum rule presents accurate results which are the closest to our proposal. The worst values of CRR at Rank-one are related to the individual source Fast-Hessian with 96.86% on the CASIA-IrisV4-Interval database, the individual source Hessian-Laplacian with 87.92% on the MMU 2 database, and the individual source Fast-Hessian with 76.26% on the UBIRIS 1 database.

Overall, we can observe that the best results are obtained on the CASIA-IrisV4-Interval database. This is mostly due to the fact that CASIA-IrisV4-Interval database presents well contrasted images with adequate resolution for keypoint-based feature extraction methods although this database is strongly disrupted by eyelid and eyelash occlusions. The MMU 2 and UBIRIS 1 databases have less image resolution. The UBIRIS 1 database is more noised in terms of illumination, motion blur, off angle, and gaze direction. Therefore, we claim that our method has the most stable and the highest performance level on the three considered databases. Also, we can demonstrate the advantages of use the proposal if we compare the final results versus the ones reported in Table 5. Finally, we can confirm the suitability of the proposed fusion scheme to combine the discriminatory power from the three used information sources.

4.3.1. Comparison with state-of-the-art algorithms

In this section, we attempt to establish a comparison between our proposed method and state-of-the-art algorithms. A reference study [45] provides a summary of the most used reference softwares for comparison purposes. To this end, we have used partial codes of some of these reference softwares such as: Masek's MATLAB source code [32], open source for Iris (OSIRIS) [26], and University of Salzburg Iris Toolbox (USIT) [45]. In our experiments, we have used the feature extraction module of some of these reference softwares. The Masek's MATLAB source code implements the Daugman's feature extraction approach [13] which is based on 1D Log-Gabor filters. The OSIRIS package extracts features using the Daugman approach [12] which is based on a bank of Gabor filters. With respect to the USIT software, we have used the implemented Ma's approach which is based on characterizing key local variations [31]. In addition, we used for comparison purposes two SIFT based feature extraction methods which claim robustness in non-ideal iris recognition. The first one is proposed by Belcher and Du [6] and consists of a region-based SIFT approach. The second one presented by Alonso et al. [2] combines SIFT based features and Log-Gabor wavelets-based

Please cite this article as: Y. Alvarez-Betancourt, M. Garcia-Silvente, A keypoints-based feature extraction method for iris recognition under variable image quality conditions, Knowledge-Based Systems (2015), http://dx.doi.org/10.1016/j.knosys.2015.10.024

Table 6
Comparison of performance measures with state-of-the-art algorithms for each database. Best result in bold.

CASIA-IrisV4-Interval				
	AUC	EER	GAR at FAR = 0.00%	CRR at Rank-one
Belcher [6]	98.12 ± 0.004	5.94 ± 0.003	60.45 ± 0.018	75.76 ± 0.003
Ma [31]	96.61 ± 0.473	5.66 ± 0.005	88.30 ± 0.007	87.77 ± 0.002
Daugman [12]	98.47 ± 0.282	4.30 ± 0.005	81.84 ± 0.017	82.34 ± 0.006
Daugman [13]	99.45 ± 0.162	1.68 ± 0.003	96.41 ± 0.001	96.83 ± 0.003
Alonso [2]	99.63 ± 0.002	1.37 ± 0.003	97.27 ± 0.004	96.95 ± 0.005
Proposed method	**99.90 ± 0.159**	**0.55 ± 0.003**	**98.50 ± 0.003**	**99.20 ± 0.007**
	MMU 2			
Belcher [6]	97.80 ± 0.004	7.55 ± 0.008	52.06 ± 0.013	76.40 ± 0.014
Ma [31]	97.94 ± 0.622	5.22 ± 0.004	81.22 ± 0.009	88.50 ± 0.012
Daugman [12]	99.11 ± 0.028	3.36 ± 0.009	81.33 ± 0.008	93.66 ± 0.008
Daugman [13]	99.16 ± 0.234	3.78 ± 0.006	68.42 ± 0.017	91.12 ± 0.014
Alonso [2]	99.51 ± 0.003	3.79 ± 0.006	75.00 ± 0.015	91.64 ± 0.009
Proposed method	**99.89 ± 0.124**	**1.56 ± 0.020**	**90.43 ± 0.024**	**98.08 ± 0.022**
	UBIRIS 1			
Belcher [6]	85.83 ± 0.008	21.36 ± 0.008	10.28 ± 0.014	20.86 ± 0.021
Ma [31]	89.25 ± 0.256	17.78 ± 0.008	41.93 ± 0.039	27.89 ± 0.009
Daugman [12]	94.38 ± 0.115	12.45 ± 0.007	40.73 ± 0.009	53.18 ± 0.003
Daugman [13]	96.95 ± 0.167	8.61 ± 0.002	53.55 ± 0.004	58.61 ± 0.023
Alonso [2]	96.75 ± 0.001	8.98 ± 0.003	54.79 ± 0.006	58.67 ± 0.014
Proposed method	**99.05 ± 0.109**	**3.50 ± 0.007**	**81.60 ± 0.011**	**89.41 ± 0.029**

features at matching score level. Also, we have followed the experimentation protocol described previously to compute the performance measure of state-of-the-art algorithms. We are dealing with feature extraction after applying our iris segmentation method. Besides, we use the nearest neighbor classifier on the same data partitions at 3-fold cross validation. Table 6 presents some performance measures of our proposal and of state-of-the-art algorithms such as: AUC, EER, GAR at FAR=0.00%, and CRR at Rank-one. It is worth noting that Table 6 data are presented in ascending order by the AUC column.

As can be seen in Table 6, our feature extraction method outperforms state-of-the-art algorithms on the three iris image databases. Our proposal reaches the maximum AUC value, minimum EER value, maximum GAR at FAR=0.00% value, and maximum CRR at Rank-one value on the three databases. Our results are followed closely by the algorithms of Daugman [13] and Alonso et al. [2]. The experimental results in Table 6 point to the superiority of our proposal compared with the works considered as state-of-the-art. Besides, our proposed method is the more stable in terms of robustness under the conditions of great variability of image quality as exemplified by the three used databases. Although the past literature underlines the advantages of using keypoint-based methods for scale and rotation variations, the obtained results reveal how well our proposal performs when dealing with other quality factors such as occlusions, illumination, blur, point of view, all of which affect the used experimental databases.

In order to demonstrate the feasible use of the proposed method in relation to its efficiency, we have executed some time-consuming tests including state-of-the-art algorithms. Table 7 presents some results of these time-consuming tests measured in seconds, corresponding to the feature extraction and matching stages. They are presented in ascending order according to the time-required for feature extraction.

In the result of Table 7, we can observe the notable computational complexity required by the SIFT based feature extraction methods [2,6]. The comparison is not fair because the rest of the methods cannot deal with non-ideal irises. This stands out in our proposed method which requires more computational cost due to the fusion of SIFT based features from 3 information sources. However, the time required for the matching stage in all these SIFT based feature extraction methods (see Table 8) is equivalent to other state-of-the-art algorithms which are considered as being the most efficient. In a real application which requires comparing one individual with a large database of identities, the most important stage is the matching stage. This claim is based on the fact that the enrolled identities are saved as feature templates. Therefore, the SIFT based feature extraction methods are well suited to implement real applications. In conclusion, our proposed feature extraction method is all the more suitable because of its robustness as demonstrated by the experimentations performed under variable image quality conditions.

Taking into account the differences in time when the iris is processed using methods designed for non-ideal irises, an initial quality analysis could be included in order to determine the kind of algorithm to use.

Table 7
Comparison of feature extraction times with state-of-the-art algorithms. Best result in bold.

	CASIA-IrisV4-Interval	MMU 2	UBIRIS 1
Daugman [13]	**0.0057**	**0.0052**	**0.0042**
Ma [31]	0.0128	0.0127	0.0138
Daugman [12]	0.0164	0.0163	0.0146
Belcher [6]	0.2542	0.1472	0.1258
Alonso [2]	0.3716	0.1542	0.1488
Proposed method	0.6867	0.3347	0.2952

Table 8
Comparison of matching times with state-of-the-art algorithms. Best result in bold.

	CASIA-IrisV4-Interval	MMU 2	UBIRIS 1
Daugman [13]	**0.0062**	0.0060	0.0060
Ma [31]	0.0062	0.0062	0.0062
Daugman [12]	0.0067	0.0067	0.0066
Belcher [6]	0.0087	0.0067	0.0065
Alonso [2]	0.1303	0.0256	0.0157
Proposed method	0.0115	**0.0028**	**0.0022**

Please cite this article as: Y. Alvarez-Betancourt, M. Garcia-Silvente, A keypoints-based feature extraction method for iris recognition under variable image quality conditions, Knowledge-Based Systems (2015), http://dx.doi.org/10.1016/j.knosys.2015.10.024

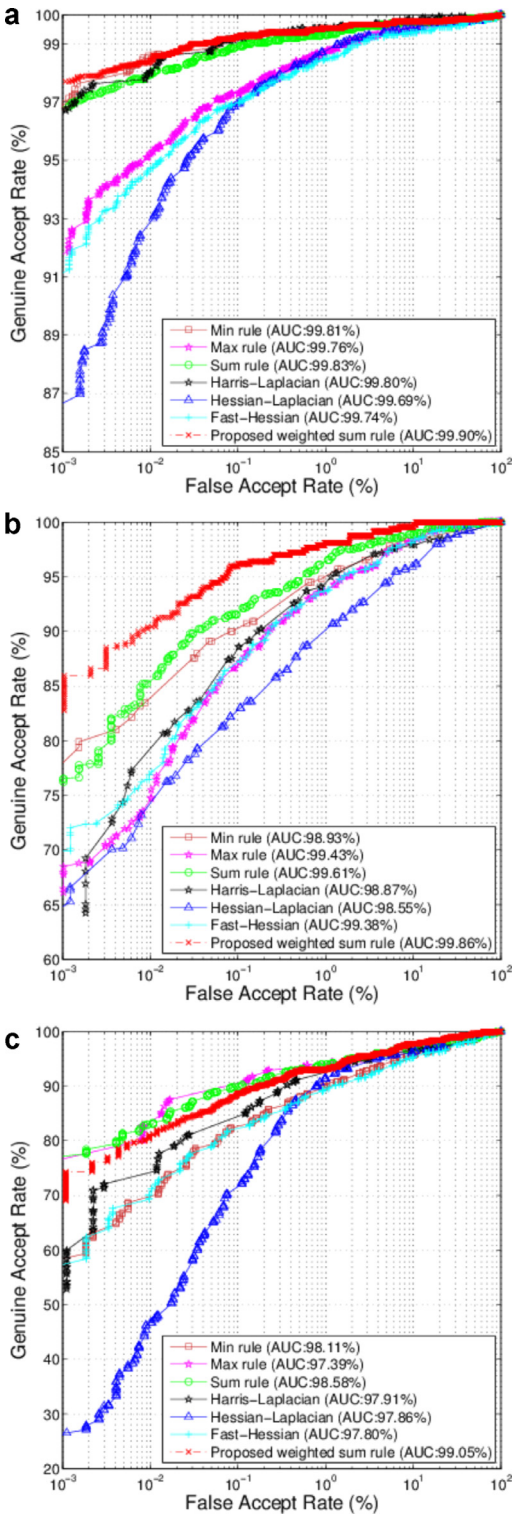

Fig. 9. Comparison using ROC curves of iris recognition with individual sources and fusion rules on different databases. (a) CASIA-IrisV4-Interval. (b) MMU 2. (c) UBIRIS 1.

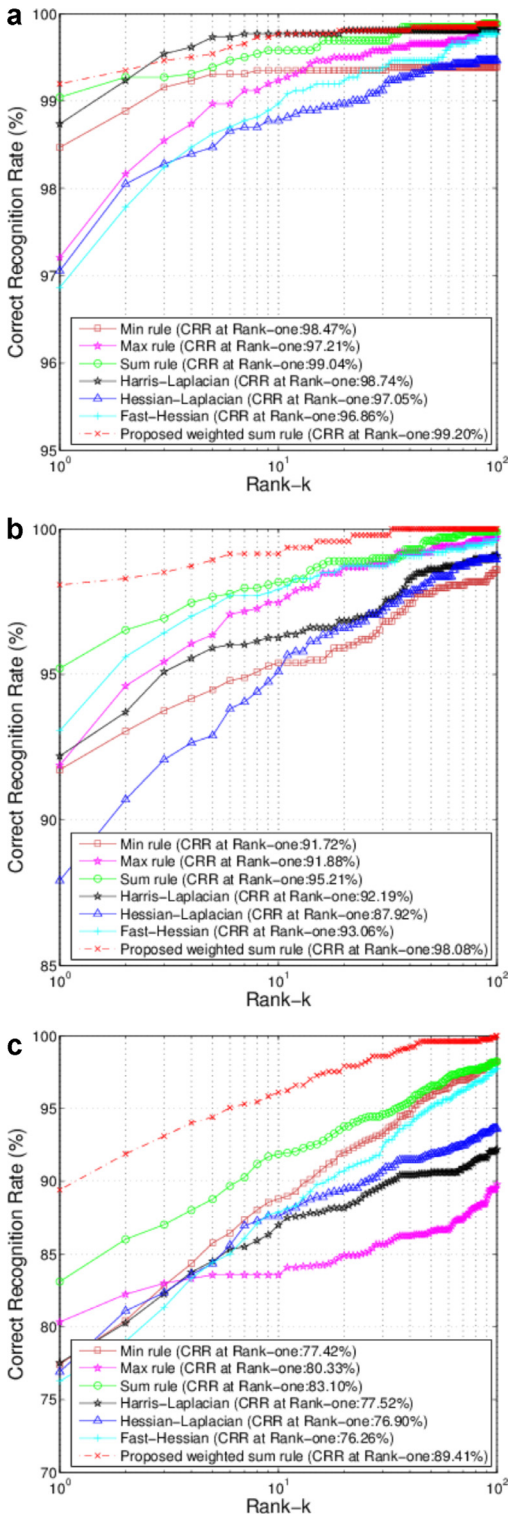

Fig. 10. Comparison using CMC curves of iris recognition with individual sources and fusion rules on different databases. (a) CASIA-IrisV4-Interval. (b) MMU 2. (c) UBIRIS 1.

5. Conclusions

In this paper, we have presented a robust keypoints-based feature extraction system for iris recognition under variable image quality conditions. Our proposal is based on the efficient fusion of three information sources of SIFT features at matching score level. This is carried out using a proposed fusion scheme which is based on the ranking of three well-known performance measures (AUC, EER and CRR at Rank-one). This is a novelty approach which use the potentialities of SIFT features to describes other sources of keypoints and fuse them to achieve a better performance on non-ideal iris images. Our statistical analysis demonstrates the complementary as well as the discriminatory power of the individual sources when they are combined for recognition on highly or less textured iris images. Therefore, we have verified the feasible combination of the used information

Please cite this article as: Y. Alvarez-Betancourt, M. Garcia-Silvente, A keypoints-based feature extraction method for iris recognition under variable image quality conditions, Knowledge-Based Systems (2015), http://dx.doi.org/10.1016/j.knosys.2015.10.024

sources. The proposal has been tested using three databases which, as a whole, constitute a perfect example of variable image quality conditions. The results indicate that the performance of the proposal tends to decline in the case of images with low resolution. The best results were obtained on the CASIA-IrisV4-Interval database. This is not surprising since this database consists of images in which the iris region bigger than the iris region of images from both MMU 2 and UBIRIS 1. Keypoints-based methods require an adequate amount of information to represent in a reliable way the discriminatory information of the acquired images. Besides, we have demonstrated the superiority of the proposed feature extraction method in relation to state-of-the-art algorithms in both verification and identification modes. Although the feature extraction stage of our proposal is time-consuming, the matching stage is very short as we can see when comparing the time required by our method with the state-of-the-art algorithms. Therefore, we can conclude that our proposal is suitable to implement real-time applications of person recognition.

Acknowledgments

The authors would like to thank Dr. Eduardo Concepción-Morales and Dr. Dominique Lepicq for their important comments on the development of this paper. Also, we want to thank the anonymous reviewers for the important comments provided. Besides, we want to thank the Chinese Academy of Sciences Institute of Automation (China), Multimedia University (Malaysia), and SOCIA Lab at the University of Beira Interior (Portugal) for providing the iris databases used in this work. This work was supported by the Andalusian Regional Government Project P09-TIC-04813, the Spanish Government Project TIN2012-38969 and the AUIP.

References

[1] E. Akbari, H.M. Dahlan, R. Ibrahim, H. Alizadeh, Hierarchical cluster ensemble selection, Eng. Appl. Artif. Intell. 39 (2015) 146–156.
[2] F. Alonso-Fernandez, P. Tome-Gonzalez, V. Ruiz-Albacete, J. Ortega-Garcia, Iris recognition based on sift features, in: Proceedings of the 2009 1st IEEE International Conference on Biometrics, Identity and Security, BIdS 2009, 2009.
[3] Y. Alvarez-Betancourt, M. Garcia-Silvente, A fast iris location based on aggregating gradient approximation using QMA-OWA operator, in: Proceedings of the 2010 IEEE World Congress on Computational Intelligence, WCCI 2010, 2010, pp. 1–8.
[4] Y. Alvarez-Betancourt, M. Garcia-Silvente, An overview of iris recognition: a bibliometric analysis of the period 2000–2012, Scientometrics 101 (3) (2014) 1–31.
[5] H. Bay, A. Ess, T. Tuytelaars, L.V. Gool, Speeded-up robust features (surf), Int. J. Comput. Vis. Image Underst. 110 (3) (2008) 346–359.
[6] C. Belcher, Y. Du, Region-based sift approach to iris recognition, Opt. Lasers Eng. 47 (1) (2009) 139–147.
[7] S. Bharadwaj, H.S. Bhatt, M. Vatsa, R. Singh, Periocular biometrics: when iris recognition fails, in: Proceedings of the 4th IEEE International Conference on Biometrics: Theory, Applications and Systems, BTAS 2010, 2010.
[8] W. Boles, B. Boashash, A human identification technique using images of the iris and wavelet transform, IEEE Trans. Signal Process. 46 (4) (1998) 1185–1188.
[9] K.W. Bowyer, K. Hollingsworth, P.J. Flynn, Image understanding for iris biometrics: a survey, Comput. Vis. Image Underst. 110 (2) (2008) 281–307.
[10] R. Chen, X. Lin, T. Ding, Liveness detection for iris recognition using multispectral images, Pattern Recognit. Lett. 12 (33) (2012) 1513–1519.
[11] S. Chowhan, G. Shinde, Evaluation of statistical feature encoding techniques on iris images, in: Proceedings of WRI World Congress on Computer Science and Information Engineering, vol. 7, March 2009, pp. 71–75.
[12] J. Daugman, Biometric personal identification system based on iris analysis, US Patent No. 5,291,560, 1994.
[13] J. Daugman, How iris recognition works, in: IEEE International Conference on Image Processing, vol. 1, 2002, pp. I/33–I/36.
[14] J. Daugman, How iris recognition works, IEEE Trans. Circuits Syst. Video Technol. 14 (1) (2004) 21–30.
[15] Y. Du, C. Belcher, Z. Zhou, Scale invariant gabor descriptor-based noncooperative iris recognition, EURASIP J. Adv. Signal Process. 2010 (2010) 936512, doi:10.1155/2010/936512.
[16] J. Gan, Y. Liang, Applications of wavelet packets decomposition in iris recognition, in: Proceedings of International Conference on Biometrics, January 2006, pp. 443–449.
[17] A. González, G. Villalonga, J. Xu, D. Vázquez, J. Amores, A.M. López, Multiview random forest of local experts combining RGB and lidar data for pedestrian detection, in: Proceedings of IEEE Intelligent Vehicles Symposium, 2015.
[18] Z. He, T. Tan, Z. Sun, X. Qiu, Toward accurate and fast iris segmentation for iris biometrics, IEEE Trans. Pattern Anal. Mach. Intell. 31 (9) (2009) 1670–1684.
[19] J. Huang, C. Ling, Using auc and accuracy in evaluating learning algorithms, IEEE Trans. Knowl. Data Eng. 17 (3) (2005) 299–310.
[20] Y.-P. Huang, S.-W. Luo, E.-Y. Chen, An efficient iris recognition system, in: Proceedings of International Conference of Machine Learning and Cybernetics, Vol. 1, November 2002, pp. 450–454.
[21] A. Jain, K. Nandakumar, A. Ross, Score normalization in multimodal biometric systems, Pattern Recognit. 38 (2005) 2270–2285.
[22] A. Jain, A. Ross, S. Prabhakar, An introduction to biometric recognition, IEEE Trans. Circuits Syst. Video Technol. 14 (1) (2004) 4–20.
[23] N. Jankowski, M. Grochowski, Comparison of instances seletion algorithms. I. Algorithms survey, Proceedings of ICAISC 2004, LNAI, vol. 3070, Springer-Verlag, Berlin, Heidelberg, 2004, pp. 598–603.
[24] N.D. Kalka, J. Zuo, N.A. Schmid, B. Cukic, Estimating and fusing quality factors for iris biometric images, IEEE Trans. Syst. Man Cybern. Part A: Syst. Hum. 40 (3) (2010) 509–524.
[25] J. Kittler, M. Hatef, R. Duin, J. Matas, On combining classifiers, IEEE Trans. Pattern Anal. Mach. Intell. 20 (3) (1998) 226–239.
[26] E. Krichen, B. Dorizzi, Z. Sun, S. Garcia-Salicetti, Iris Recognition, Springer, New York, 2009.
[27] P. Li, H. Ma, Iris recognition in non-ideal imaging conditions, Pattern Recognit. Lett. 33 (8) (2012) 1012–1018.
[28] S. Li, A.K. Jain (Eds.), Encyclopedia of Biometrics, Springer, US, 2009.
[29] D. Lowe, Distinctive image features from scale-invariant keypoints, Int. J. Comput. Vis. 60 (2) (2004) 91–110.
[30] L. Ma, T. Tan, Y. Wang, D. Zhang, Personal identification based on iris texture analysis, IEEE Trans. Pattern Anal. Mach. Intell. 25 (12) (2003) 1519–1533.
[31] L. Ma, T. Tan, Y. Wang, D. Zhang, Efficient iris recognition by characterizing key local variations, IEEE Trans. Image Process. 13 (6) (2004) 739–750.
[32] L. Masek, P. Kovesi, Matlab Source Code for a Biometric Identification System Based on Iris Patterns, The School of Computer Science and Software Engineering, The University of Western Australia, 2003. http://staffhome.ecm.uwa.edu.au/~00011811/studentprojects/libor/sourcecode.html
[33] J.R. Matey, O. Naroditsky, K. Hanna, R.A.Y. Kolczynski, D.J. Loiacono, S. Mangru, M. Tinker, W.Y. Zhao, Iris on the move: acquisition of images for iris recognition in less constrained environments, Proc. IEEE 94 (11) (2006) 1936–1946.
[34] H. Mehrotra, B. Majhi, P. Gupta, Robust iris indexing scheme using geometric hashing of sift keypoints, J. Netw. Comput. Appl. 33 (3) (2010) 300–313.
[35] H. Mehrotra, B. Majhi, P. Sa, Unconstrained iris recognition using f-sift, in: Proceedings of ICICS 2011 – 8th International Conference on Information, Communications and Signal Processing, 2011.
[36] K. Mikolajczyk, C. Schmid, Scale & affine invariant interest point detectors, Int. J. Comput. Vis. 60 (1) (2004) 63–86.
[37] K. Mikolajczyk, C. Schmid, A performance evaluation of local descriptors, IEEE Trans. Pattern Anal. Mach. Intell. 27 (10) (2005) 1615–1630.
[38] K. Miyazawa, K. Ito, T. Aoki, K. Kobayashi, H. Nakajima, An efficient iris recognition algorithm using phase-based image matching, in: Proceedings of International Conference on Image Processing, 2005, pp. 49–52.
[39] K. Miyazawa, K. Ito, T. Aoki, K. Kobayashi, H. Nakajima, An effective approach for iris recognition using phase-based image matching, IEEE Trans. Pattern Anal. Mach. Intell. 30 (10) (2008) 1741–1756.
[40] D.M. Monro, S. Rakshit, D. Zhang, Dct-based iris recognition, IEEE Trans. Pattern Anal. Mach. Intell. 29 (4) (2007) 586–595.
[41] H. Parvin, M. MirnabiBaboli, H. Alinejad-Rokny, Proposing a classifier ensemble framework based on classifier selection and decision tree, Eng. Appl. Artif. Intell. 37 (2015) 34–42.
[42] H. Proença, L. Alexandre, Iris recognition: an analysis of the aliasing problem in the iris normalization stage, in: Proceedings of 2006 International Conference on Computational Intelligence and Security, ICCIAS 2006, vol. 2, 2007a, pp. 1771–1774.
[43] H. Proença, L. Alexandre, Toward noncooperative iris recognition: A classification approach using multiple signatures, IEEE Trans. Pattern Anal. Mach. Intell. 29 (4) (2007b) 607–612.
[44] A.D. Rahulkar, R.S. Holambe, Partial iris feature extraction and recognition based on a new combined directional and rotated directional wavelet filter banks, Neurocomputing 81 (2012) 12–23.
[45] C. Rathgeb, A. Uhl, P. Wild, Iris Biometrics. From Segmentation to Template Security, Springer Science+Business Media, LLC, 2013.
[46] A. Ross, K.N.A. Jain, Handbook of Multibiometrics, 1st edition, Springer, New York, USA, 2006.
[47] A. Ross, M. Sunder, Block based texture analysis for iris classification and matching, in: Proceedings of 2010 IEEE Computer Society Conference on Computer Vision and Pattern Recognition Workshops, CVPRW, 2010, pp. 30–37.
[48] K. Roy, P. Bhattacharya, Optimal features subset selection using genetic algorithms for iris recognition, in: Lecture Notes in Computer Science (including subseries Lecture Notes in Artificial Intelligence and Lecture Notes in Bioinformatics) 5112 LNCS, 2008, pp. 894–904.
[49] K. Roy, P. Bhattacharya, C. Suen, Towards nonideal iris recognition based on level set method, genetic algorithms and adaptive asymmetrical svms, Eng. Appl. Artif. Intell. 24 (3) (2011) 458–475.
[50] K. Roy, P. Bhattacharya, C.Y. Suen, Iris segmentation using game theory, Signal Image Video Process. 6 (2012) 301–315.
[51] C. Sanchez-Avila, R. Sanchez-Reillo, Two different approaches for iris recognition using gabor filters and multiscale zero-crossing representation, Pattern Recognit. 38 (2) (2005) 231–240.
[52] C. Sanchez-Avila, R. Sanchez-Reillo, D. De Martin-Roche, Iris-based biometric recognition using dyadic wavelet transform, IEEE Aerosp. Electron. Syst. Mag. 17 (10) (2002) 3–6.

Please cite this article as: Y. Alvarez-Betancourt, M. Garcia-Silvente, A keypoints-based feature extraction method for iris recognition under variable image quality conditions, Knowledge-Based Systems (2015), http://dx.doi.org/10.1016/j.knosys.2015.10.024

[53] C. Sanderson, K.K. Paliwal, Information Fusion and Person Verification Using Speech and Face Information, Research Paper IDIAP-RR, IDIAP, 02–33, 2002.
[54] G. Santos, E. Hoyle, A fusion approach to unconstrained iris recognition, Pattern Recognit. Lett. 33 (8) (2012) 984–990.
[55] D.J. Sheskin, Handbook of Parametric and Nonparametric Statistical Procedures, Chapman & Hall/CRC, 2004.
[56] S. Sun, S. Yang, L. Zhao, Noncooperative bovine iris recognition via sift, Neurocomputing 120 (2013) 310–317.
[57] Z. Sun, T. Tan, Ordinal measures for iris recognition, IEEE Trans. Pattern Anal. Mach. Intell. 31 (12) (2009) 2211–2226.
[58] C.-L. Tisse, L. Martin, L. Torres, M. Robert, Person identification technique using human iris recognition, in: Proceedings of Conference on Vision Interface, 2002, pp. 294–299.
[59] T. Tuytelaars, K. Mikolajczyk, Local invariant feature detectors: a survey, Found. Trends Comput. Graph. Vis. 3 (3) (2007) 177–280.
[60] P. Verlinde, G. Chollet, M. Acheroy, Multi-modal identity verification using expert fusion, Inf. Fusion 1 (2000) 17–33.
[61] P. Yao, J. Li, X. Ye, Z. Zhuang, B. Li, Iris recognition algorithm using modified log-gabor filters, in: Proceedings of International Conference on Pattern Recognition, August 2006, pp. 461–464.
[62] X. Zhang, C. Liu, Image annotation based on feature fusion and semantic similarity, Neurocomputing Part C 149 (2015) 1658–1671.
[63] Z. Zhiping, H. Maomao, S. Ziwen, An iris recognition method based on 2DWPCA and neural network, in: Proceedings of Chinese Control and Decision Conference (CCDC 09), June 2009, pp. 2357–2360.
[64] K. Zuiderveld, Contrast limited adaptive histograph equalization, Graphic Gems IV, Academic Press Professional, San Diego, 1994, pp. 474–485.

Please cite this article as: Y. Alvarez-Betancourt, M. Garcia-Silvente, A keypoints-based feature extraction method for iris recognition under variable image quality conditions, Knowledge-Based Systems (2015), http://dx.doi.org/10.1016/j.knosys.2015.10.024